

Article

Thermal Oxidation of Polyolefins by Mild Pro-Oxidant Additives Based on Iron Carboxylates and Lipophilic Amines: Degradability in the Absence of Light and Effect on the Adhesion to Paperboard

Tuan-Anh Nguyen ^{1,*}, Øyvind Weiby Gregersen ¹ and Ferdinand Männle ^{2,*}

¹ Department of Chemical Engineering, Norwegian University of Science and Technology, N-7491 Trondheim, Norway; E-Mail: oyvind.gregersen@chemeng.ntnu.no

² Synthesis and Properties, SINTEF Materials and Chemistry, N-0314 Oslo, Norway

* Authors to whom correspondence should be addressed;

E-Mails: ferdinand.maennle@sintef.no (F.M.); tuananh210281@gmail.com (T.-A.N.);

Tel.: +47-98-28-2491 (F.M.); +47-40-30-8660 (T.-A.N.).

Academic Editor: Philipp Vana

Received: 14 June 2015 / Accepted: 5 August 2015 / Published: 17 August 2015

Abstract: Marine and inland pollution by non-degradable plastic bags and other plastic articles is a topic of great concern. Natural degradation processes based on oxidation of plastic pollutants could possibly contribute to limit the extent of pollution. Thermal degradation of polyolefins in the absence of light by non-polluting pro-oxidants has not been presented before. In this study, we show that two amines, stearyl amine and [(3-(11-aminoundecanoyl) amino) propane-1-] silsesquioxane (amino-POSS) in combination with ferric stearate (FeSt₃) tremendously accelerate the thermal oxidation of polyolefins compared with reference samples. Both amines and FeSt₃ are to a large extent based on renewable resources. Polyethylene and polypropylene samples containing less than 100 ppm of iron and 1% of amine were extremely brittle after 10 days in a circulation oven in the absence of light. No significant degradation could be seen with samples containing iron but no amine. In a different application, the initial oxidation of polyethylene can be used in order to increase its adhesion to cardboard. Excellent adhesion between polyethylene and cardboard is important for liquid packaging based on renewable resources. Amino-POSS has been chosen for food packaging applications due to its expected lower leakage from polyethylene (PE) compared with stearyl amine. Film samples of PE/amino-POSS/FeSt₃ blends were partly oxidized in a circulation oven. The oxidation was documented by

increased carbonyl index (CI) and melt flow index (MFI). The limited extent of oxidation has been proved by unchanged tensile strength and only moderate changes in elongation at break when compared to reference polyethylene films containing no FeSt₃ or amino-POSS. The PE/amino-POSS/FeSt₃ blends were compression moulded to paperboard. The adhesion of non-aged blends to paperboard decreased with increasing amino-POSS content which is in good compliance with an earlier reported lubricant effect of high amounts of POSS in PE. Thermal ageing of PE/amino-POSS/FeSt₃ films prior to coating however led to a significant increase in adhesion. Improved physical interlocking due to increased MFI and interaction between C=O of the blends and OH of paperboard can explain the adhesion improvement. The films were not brittle after thermal ageing, which makes their use in industrial packaging feasible. A mechanism explaining the role of amines during thermal oxidation of polyolefins in the presence of iron is proposed.

Keywords: polyethylene; pro-oxidant; amino-POSS; adhesion strength; carbonyl index; thermal ageing

1. Introduction

Polyethylene (PE) coated paperboard has been widely applied for packaging foods, beverages and pharmaceuticals because of its low cost, lightweight, non-toxicity, excellent water barrier, good mechanical properties and processability. Adhesion strength between PE and paperboard is an important property of such packaging materials [1]. The adhesion was successfully improved by introducing polar groups such as CO and OH on the surface of PE by oxidative treatment prior to laminating with paperboard [2,3]. Limited oxidation of PE can be provided by mixing pro-oxidant additives into PE. Pro-oxidant additives such as stearate salt of iron, cobalt or manganese are often used to improve the degradability of PE by oxidation [4–7]. The rate-limiting step in the oxidation of PE mediated by pro-oxidant additives is the decomposition of hydroperoxides. Cobalt and manganese yield sufficient thermal oxidation rates in the absence of UV light. This is however not the case with iron [8]. The decomposition of hydroperoxides in polyethylene by iron alone is not fast enough to provide rapid thermal oxidation of the polymer. However, suitable accelerators could increase the decomposition of hydroperoxides in PE and thus yield rapid thermal oxidation rates with iron as the only transition metal present. Amines are known to act as decomposer of hydroperoxides [9–12]. Amines could therefore act as suitable accelerators for iron containing prodegradants.

The application of amines in polyethylene packaging requires food contact approval and no significant colour or odour contribution from the amine component. Additionally, the amine has to be soluble or easily dispersible in the polyethylene matrix. Amines derived from fatty acids, such as stearyl amine or polymer based amines are therefore suitable candidates in order to accelerate the rate of thermal oxidation rate in polyethylene containing an iron based pro-oxidant.

Many studies have reported that the oxidation of the PE films containing pro-oxidant additive prevalently produces carbonyl (C=O) on its surface [6,13–19]. The presence of carbonyl group on PE film surface can lead to an increase in its surface polarity. When such film is laminated with paperboard,

the adhesion can be improved due to an increase in the interfacial attractive force [20–22]. By using iron-based pro-oxidants in combination with stearyl amine or polymer based amines, it should therefore be possible to improve the adhesion of polyethylene to paperboard.

An interesting group of polymeric amines are based on polyhedral oligomeric silsesquioxane (POSS). POSS is an inorganic-organic hybrid compound with a general formula $(\text{RSiO}_{1.5})_n$, where R is an organic group, n is the number of silicon atoms ($n = 8, 10, 12$), and a special molecular structure which is composed of an inorganic core cage and the functional organic group surrounding the core cage. The organic groups allow POSS compounds to be easily incorporated into organic polymers [23,24]. POSS has recently been used in thermoplastics and improve several properties of the materials [25–33]. In our previous work, small amounts of bio-POSS octa-(ethyl octadeca 10,13-dienoamide silsesquioxanes) was added to polyethylene (PE) and laminated with paperboard. The adhesion property of this packaging material was successfully improved when small amounts of POSS have been used. With increasing POSS amounts, the adhesion between polyethylene and paperboard was decreased, most likely due to the lubricant effect of the fatty amide based POSS [34]. We have previously based on commodities such as 3-aminopropyltriethoxy silane and fatty acids. The use of commodities in POSS synthesis provides a significantly improved cost/benefit when compared with POSS synthesis, which is based on silanes alone. A high solids air drying paint, where amide substituted POSS is an essential part of the binder system has been commercialized [35].

In this work, we chose stearyl amine to investigate the oxidation of polyethylene and polypropylene by iron/amine pro-oxidants in the first part. In the second part, we chose [(3-(11-aminoundecanoyl) amino) propane-1-] silsesquioxane (amino-POSS) to examine the effect on the adhesion strength of PE films iron/amine pro-oxidants to paperboard. Amino-POSS is due to its structure and molecular weight is likely to show lower leakage from PE compared with stearyl amine. It is therefore the preferred amine for food packaging applications.

2. Experimental Section

2.1. Materials

Low density polyethylene powder (LDPE) was provided by Normatch AS, Gjerdrum, Norway, with a melting point of 110 °C, a melt flow index (MFI) of 20 g/10 min (190 °C/2.16 kg) and a broad molecular weight distribution. According to the manufacturer, no anti-oxidant, no technical additive, and no catalyst residue are present in this LDPE quality. The pro-oxidant additives were two masterbatches of ferric stearate (FeSt_3) in polyethylene and provided by Nor-X Industry AS (Gursken, Norway). Masterbatch A had an iron content of 0.36% and Masterbatch B had an iron content of 0.38%. Both masterbatches contain stearic acid in addition to iron (III) stearate. The concentration of stearic acid in Masterbatch B is about twice as high as in Masterbatch A. Paperboard was provided by Korsnäs AB (Frövi, Sweden). Stearyl amine was purchased from Aldrich (St. Louis, MO, USA).

2.1.1. POSS Compound

The POSS compound is [(3-(11-aminoundecanoyl) amino) propane-1-] silsesquioxane or amino-POSS. It was previously synthesized in our laboratory by a two-step procedure [35].

In the first step 3-aminopropyltriethoxy silane was converted to amino functionalized POSS by a sol-gel process. In the second step, the amine groups were further modified by an amino acid (11-aminoundecanoic acid). A typical structure of amino-POSS is shown in Figure 1.

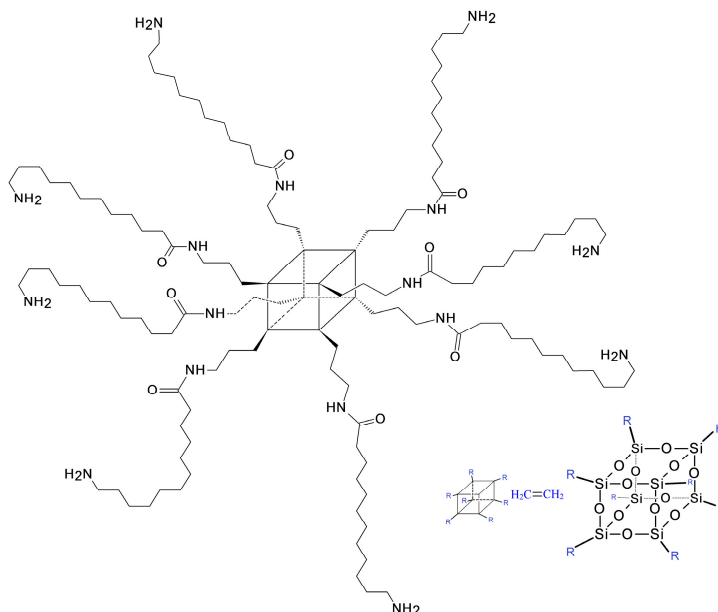


Figure 1. Typical structure of [3-(11-aminoundecanoyl amino) propane-1-] silsesquioxane (amino-POSS).

2.1.2. Paperboard

The paperboard has two sides with different colours: An uncoated side (brown) and a pre-coated side (white) (Figure 2a); Figure 2b shows a scanning electron microscopy (SEM) image of the uncoated side of the paperboard.

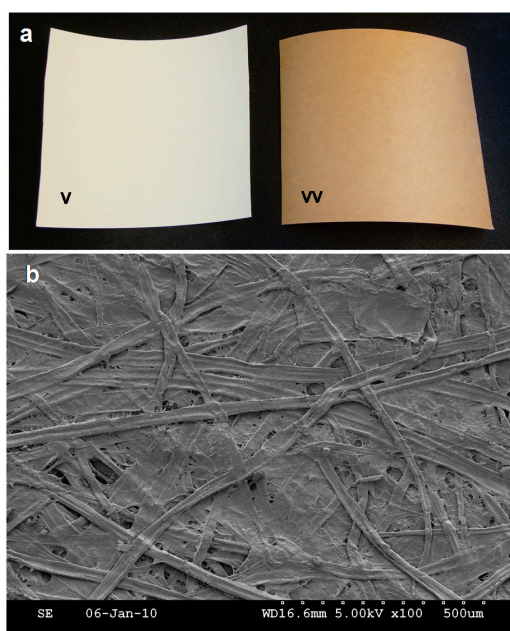


Figure 2. (a) Two sides of paperboard: (v) pre-coated side and (vv) uncoated side; (b) SEM images of the uncoated side of the paperboard.

The uncoated side of paperboard is very rough, containing large fibres. There are many pinholes and depressions on the uncoated side of the paperboard. As can be observed, the uncoated side of paperboard is very rough, containing large fibres. The rough surface of the uncoated side of paperboard is very advantageous for polymer coating mechanical adhesion.

2.1.3. Amine Masterbatches

Amino-POSS was dried at 120 °C to fully remove solvent 2-butoxy ethanol which was used in its synthesis. Masterbatch C was prepared in a twin screw 15 cc micro extruder (DSM; Royal DSM: Heerlen, The Netherlands) including 90 wt% PE powder and 10 wt% dried amino-POSS.

Masterbatch D was prepared by the same procedure and consists of 90 wt% PE powder and 10 wt% stearyl amine.

2.2. Sample Preparation

2.2.1. Preparation of PE and PP Film Containing Iron/Stearyl Amine Proxidant

Mixtures of PP or PE and different masterbatches were compounded for three minutes in the twin screw 15 cc micro extruder (DSM MIDI2000; Xplore Instruments: Geleen, The Netherlands) at 230 °C. The mixtures were compression moulded on a hydraulic compressor (Fontijne TH200; Fontijne Grotnes: Vlaardingen, The Netherlands) to a film thickness of 0.1 mm. The temperature of the top and bottom plates of the hydraulic compressor was 180 °C, the pressure was 10 MPa, and the total compression time was 5 min. Samples suitable for mechanical testing with “dumbbell” shape were prepared by using an appropriate sample puncher (Zwick & Co. KG: Ulm, Germany). The samples had a total length of 67 mm, a width at both ends of 14 mm and a width in the elongation zone of 5 mm. Table 1 shows the composition of the different mixtures.

Table 1. Compositions of PE or PP mixtures with iron/stearyl amine proxidant ([%] as [wt%]; masterbatch A, B and D were described in Section 2.1).

Sample Mixture	Iron Masterbatch [%]	Amine Masterbatch [%]	Polyolefin [%]	Iron [ppm]	Amine [%]
PP-1	A [2%]	0	PP [98%]	72	0
PP-2	A [5%]	0	PP [5%]	180	0
PP-4	A [2%]	D [10%]	PP [88%]	72	1
PP-8	B [2%]	0	PP [98%]	76	0
PE-9	B [2%]	0	PE [98%]	76	0
PE-12	B [2%]	D [10%]	PE [98%]	76	1

2.2.2. Preparation of PE and PE/Amino-POSS/FeSt₃ Film

Mixtures of PE, Masterbatch A and Masterbatch C were blended by melt mixing in different ratios (see Table 2) in which the content of FeSt₃ was constantly kept at 0.5 wt% for all samples. The extrusion temperature of two processes was constantly kept at 180 °C from hopper to die section of micro-extruder,

the operating screw speed was controlled at 50 rpm/min and the resident time distribution profile was 5 min. The blend product was cut into pellets.

Table 2. Compositions of PE/Amino-POSS/FeSt₃/blends ([%] as [wt%], mb: masterbatch).

Sample Code	PE (pellet) (wt%)	mb A (wt%)	mb C (wt%)	Composition		
				PE [%]	Fe [ppm]	amino-POSS [%]
PE	100	0	0	100	0	0
90505	90	5	5	99	180	0.5
85510	85	5	10	98.5	180	1
80515	80	5	15	98	180	1.5

Thin films of PE and the blends were prepared by compression moulding pure PE powder and PE/amino-POSS/FeSt₃ pellets on a hydraulic compressor (Fontijne TH200; Fontijne Grotnes: Vlaardingen, The Netherlands), respectively. The film thickness was 0.1 mm. The temperature of the top and bottom plates of the hydraulic compressor was 180 °C, the pressure was 10 MPa, and total time was 5 min.

2.2.3. Thermal Ageing of the Film

The dumbbell shape samples with the compositions from Table 1 were thermally exposed at 80 °C for 5 or 10 days in an air circulation oven (Termaks 4057; Termaks AS: Bergen, Norway).

The films with the compositions from Table 2 were thermally exposed at 70 °C for 3 or 6 days in an air circulation oven (Termaks 4057; Termaks AS: Bergen, Norway).

2.2.4. Coating on Paperboard

The films with the compositions from Table 2 and the respective thermal ageing were coated on paperboard by compression moulding coating on a hydraulic compressor (Fontijne TH200; Fontijne Grotnes: Vlaardingen, The Netherlands). The coating conditions were kept constant at the pressure of 10 MPa and the temperature of the top/bottom plate of 200 °C/20 °C. The coating process was complete after cooling down two plates of the compressor to the room temperature by opening cold water system. The coating time was 3 min.

2.3. Characterization

2.3.1. Tensile Testing of Dumbbell Shape Samples and Respective Thermal Ageing

The mechanical properties of the dumbbell shape samples were determined by tensile testing according to ISO 527-1 on the device Zwick-Z250 (Zwick International: Ulm, Germany). At least 5 specimens of each film were prepared for tensile testing. The test was run at the speed of 50 mm/min and room temperature.

2.3.2. ATR-FTIR and Carbonyl Index (CI)

Attenuated total reflection Fourier transform infrared (ATR-FTIR) was performed in a PerkinElmer FTIR device (Spectrum One) at room temperature in the wave number range 650–4000 cm^{-1} , at a resolution of 4 cm^{-1} , and scan number of 4. The result spectrum was reported as absorbance unit (a.u.).

Results from ATR-FTIR analysis were used to determine the carbonyl index (CI). CI is a measurement of the amount of carbonyl compounds formed during the thermal oxidation and is calculated as the ratio of the absorbance (A) of carbonyl peak in the region 1700–1780 cm^{-1} and the CH_2 scissoring peak at 1464 cm^{-1} [13–15]:

$$CI = \frac{A_{1700-1780 \text{ cm}^{-1}}}{A_{1464 \text{ cm}^{-1}}} \quad (1)$$

2.3.3. Adhesion Measurement

A T-peel test was performed on a tensile tester (Zwick-Z250; Zwick International: Ulm, Germany) to determine the adhesion of our samples. At least five T-type specimens (200 mm in length and 15 mm in width) were prepared for each sample by using JDC-15 mm-10 in sample cutter (Thwing-Albert, West Berlin, NJ, USA). The polymer coating was peeled at the speed of 30 mm/min. and over a length of 150 mm.

The adhesion value was determined as:

$$Adhesion = \frac{Peel \ force}{Width} \text{ (N/m)} \quad (2)$$

The adhesion strength of the sample was calculated as the average of five adhesion values that corresponded to five specimens.

2.3.4. Melt Flow Index

The effect of amino-POSS content on melt flow of PE was monitored by melt flow index (MFI) method on a melt flow apparatus, Davenport 3/80. The materials were fully loaded into a cylinder of MFI device and then melted at temperature of 190 °C. Pre-heating time and extrudate time were set at 5 and 10 min. MFI was expressed as the mass of the material per 10 min extruded through the die of 2.09 mm in diameter and 8 mm in length, under the standard weight of 2.16 kg:

$$MFI = \frac{Average \ extrudate \ weight}{Time} \text{ (g/10 min)} \quad (3)$$

2.3.5. Mechanical Properties

The mechanical properties of the film were determined by tensile testing according to ISO 527-1 on the device Zwick-Z250. Test specimens were cut from the film with “dumbbell” shape. At least 5 specimens of each film were prepared for tensile testing. The test was run at the speed of 50 mm/min and room temperature.

3. Results and Discussion

3.1. Polyolefin Samples with Iron Pro-Oxidant and Stearyl Amine Accelerator

Tensile Properties after Different Periods of Ageing

The tensile properties of PP and PE samples with iron pro-degradant and stearyl amine accelerator are shown in Tables 3 and 4. The results show clearly the influence of the stearyl amine accelerator in PP-4 and PE-12 compared with the reference sample mixtures PP-1 and PE-9. The extreme brittleness of PP-4 after 10 days at 80 °C shows that the stearyl amine accelerators can yield rapid thermal oxidation rates of polyolefins with iron as the only transition metal present. Increase of iron concentration does not give a significant increase in the thermal oxidation rate.

Comparison of PP-1 and PP-8 shows that the increased content of stearic acid (about double amount in PP-1 compared to PP-1) leads to a reduced oxidation rate.

Table 3. Elongation at break [%] after 0, 5 and 10 days of ageing at 80 °C.

Sample Mixture	0 Days	5 Days	10 Days
PP-1	652 ± 113	210 ± 165	8 ± 5
PP-2	536 ± 261	426 ± 367	13 ± 13
PP-4	868 ± 84	270 ± 286	<1 (extremely brittle)
PP-8	669 ± 242	720 ± 155	569 ± 291
PE-9	614 ± 311	355 ± 361	610 ± 331
PE-12	797 ± 103	765 ± 166	11 ± 10

Table 4. Tensile strain at break [MPa] after 0, 5 and 10 days of ageing at 80 °C.

Sample Mixture	0 Days	5 Days	10 Days
PP-1	27.1 ± 2.1	29.7 ± 0.7	22.2 ± 2.0
PP-2	27.0 ± 1.2	27.3 ± 2.7	21.7 ± 5.1
PP-4	33.5 ± 2.4	28.7 ± 2.6	<2 (extremely brittle)
PP-8	30.3 ± 1.6	32.7 ± 3.1	28.5 ± 1.5
PP-9	28.7 ± 3.6	30.1 ± 2.5	28.4 ± 1.3
PP-12	29.7 ± 6.9	27.9 ± 7.7	12.7 ± 3.0

The results also show that processing of the mixtures at the applied conditions is feasible. Elongation at break of several hundred percent clearly indicate that the samples have not been degraded during processing.

3.2. PE Samples with Iron Pro-Oxidant and Amin-POSS Accelerator

3.2.1. ATR-FTIR Studies

The ATR-FTIR is a useful technique for characterizing the surface of the material. In this work, the ATR-FTIR analyses were performed on starting materials and blends from Table 2. The result is shown in Figure 3. The study of Rao was used for the interpretation of our ATR-FTIR spectra [36].

The main peaks of PE are 2920 cm^{-1} and 2851 cm^{-1} (CH_2 stretching), 1471 cm^{-1} and 1430 cm^{-1} (CH_2 bending), 720 cm^{-1} (CH_2 rocking). The main peaks of amino-POSS are: the absorption peaks at 3287 cm^{-1} and 3074 cm^{-1} are assigned to the hydrogen-bonded N–H stretching ($\text{N–H}\cdots\text{O}=\text{C}$); two bands appear at 1640 cm^{-1} and 1548 cm^{-1} are assigned to amide I (carbonyl $\text{C}=\text{O}$) and amide II (mixed vibration involving N–H in-plane bending and C–N stretching), respectively. Normally, the intensity of amide I is stronger than that of amide II. A band at 1271 cm^{-1} is amide III (mixed vibration of C–N stretching and N–H bending). Two strong and broad bands at 1119 cm^{-1} and 1028 cm^{-1} exhibit Si–O–Si stretching of the cubic Si_8O_{12} structure. The spectrum of masterbatch FeSt_3/PE shows two strong peaks near 2920 and 2851 cm^{-1} (CH_2 stretching), a strong and sharp peak at 1700 cm^{-1} (carbonyl $\text{C}=\text{O}$ of ester group), 1471 cm^{-1} (CH_2 bending), 1430 cm^{-1} (stretching vibration of C–O group). The band characteristic to the symmetric stretching vibration of the group COO appears at 1355 cm^{-1} . The band from 1298 cm^{-1} can be assigned to the C–COO vibrations. The interpretation of ATR-FTIR spectrum of FeSt_3/PE is similar to that in other studies concerning the spectrum of carboxylate group [37–39].

As can be observed in Figure 3, the main characteristics of PE, amino-POSS and FeSt_3 were introduced into the spectra of the blends 90505, 85510, and 80515. However, the introduced peaks are very small due to the low concentration of amino-POSS and FeSt_3 in the blends.

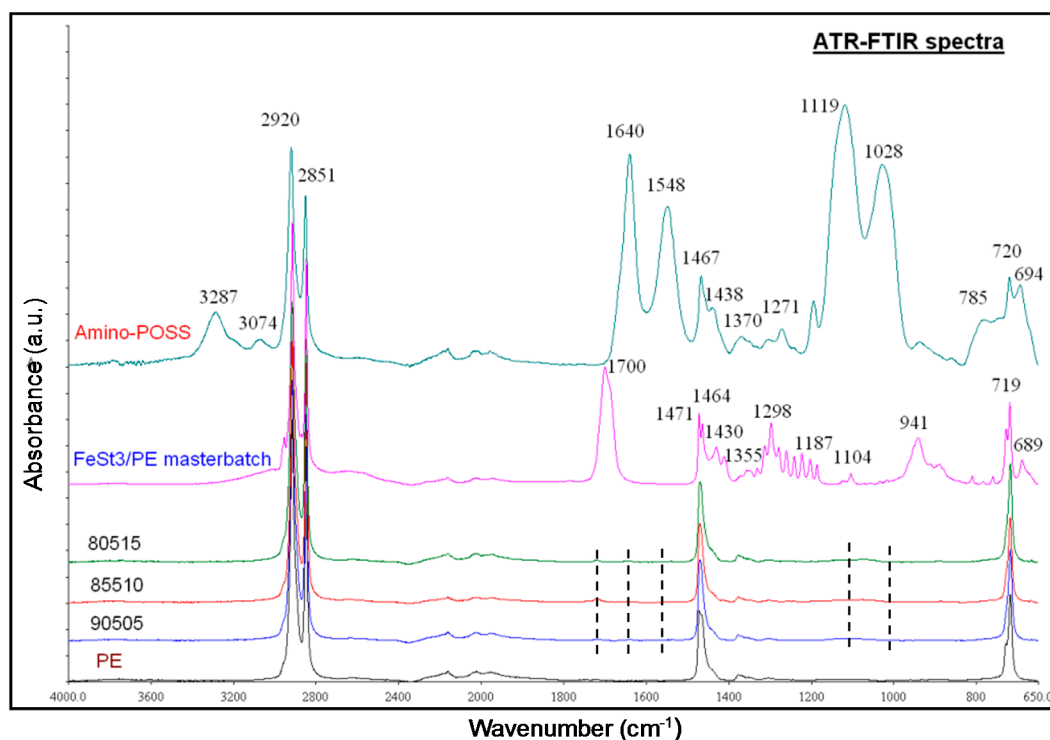


Figure 3. FTIR spectra of PE/amino-POSS/ FeSt_3 blends.

3.2.2. Thermal Ageing

The thermally aged films were characterized by ATR-FTIR and the result is shown in Figure 4. All spectra of the aged film exhibit the absorption band in the region $1700\text{--}1780\text{ cm}^{-1}$ which is assigned to carbonyl ($\text{C}=\text{O}$) groups, as determined by the overlapping bands corresponding to ester (1737 cm^{-1}), ketone (1715 and 1717 cm^{-1}). These bands are evidence for the formation of different oxidized products similar to those found in other studies involving the oxidation of PE [10,13–15]. If comparing the

intensity of C=O of the film after thermal ageing and that before ageing, it increases with increasing the ageing time.

The oxidation level of PE/amino-POSS/FeSt₃ can be evaluated by the carbonyl index (CI). Figure 5 shows the CI of PE and PE/amino-POSS/FeSt₃ film before and after thermal ageing. In general, the CI is increased with increasing the ageing time. The increase in CI of the pure PE film was negligible. The CI of the film containing pro-oxidant was higher than that of the PE film, emphasizing the degrading effect of FeSt₃. In fact, there was slight increase in the CI of the aged film 85510, 80515 whereas the CI of the film 90505 was substantially increased with increasing the ageing time. It strongly reflects that the oxidation level of the blend was limited when amino-POSS content is increased. Oxidative degradation of the blends can be detected by FT-IR even if the degree of oxidative degradation is very limited.

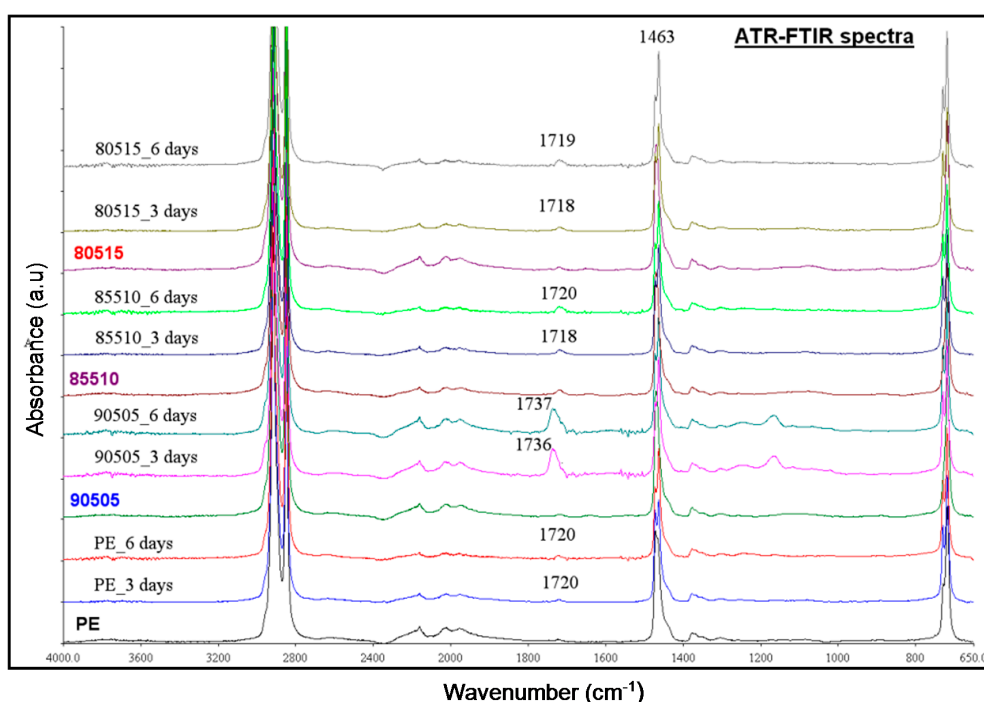


Figure 4. ATR-FTIR spectra of the blends before and after thermal ageing.

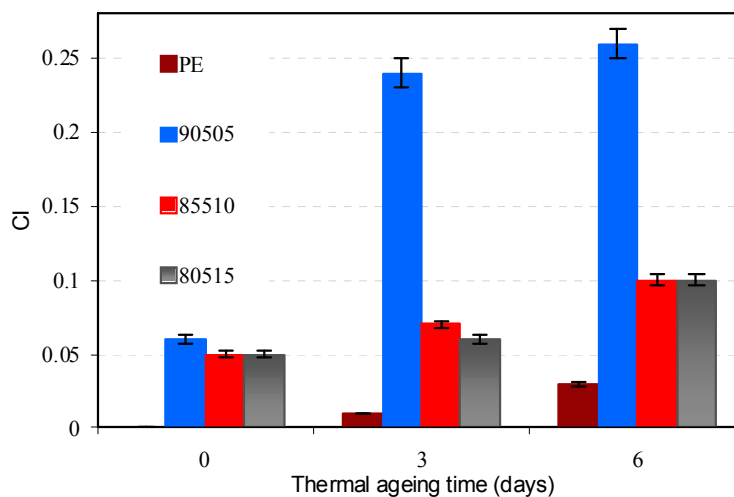


Figure 5. Carbonyl index (CI) of PE and PE/amino-POSS/FeSt₃ film.

3.2.3. Melt Flow Index (MFI)

Melt flow index is an inverse measure of the melt viscosity. The higher an MFI, the more easily the polymer flows under the test conditions. Knowing the MFI of a certain polymer is vital for controlling its processing. The melt flow properties of our PE/amino-POSS/FeSt₃ blends were determined by MFI testing and are shown in Figure 6.

Neat PE showed a decrease in the MFI after thermal ageing. It suggests that some cross-linking might have formed by oxidative degradation of PE during thermal ageing [38]. The MFI of the PE/amino-POSS/FeSt₃ blends were decreased with increasing amino-POSS content. However, after thermal ageing in air circulation oven, the MFI of the blends containing pro-oxidant additives were increased with increasing the ageing time. In fact, the increase in the MFI of the blends was negligible after three days but it was considerable after six days of air oven ageing. The blend 90505 after being thermally aged for six days exhibited the highest MFI value. It indicates that the presence of pro-oxidant leads to a chain scission of PE during thermal ageing so as to cause a change in the melt indices. The MFI of the aged blends were also decreased with increasing amino-POSS content. As determined above, the CI of the sample 90505 was much higher than that of 85510 and 80515. It indicates that the PE chain scission might be hindered by increasing amino-POSS content.

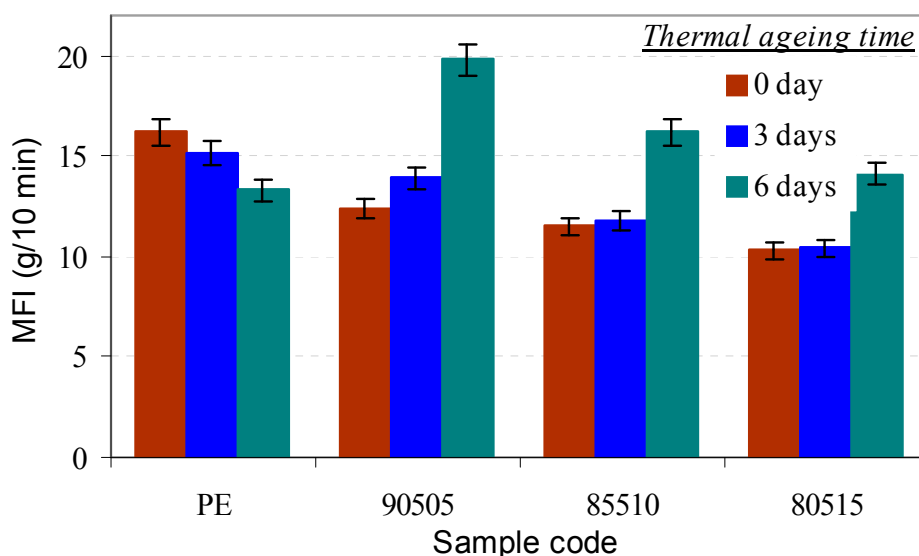


Figure 6. Melt flow index of PE and PE/amino-POSS/FeSt₃ blends after thermal aging.

3.2.4. Mechanical Properties

The mechanical properties of PE and PE/amino-POSS/FeSt₃ films were determined by tensile testing. Figure 7 illustrates the effect of thermal exposure on the tensile yield strength (σ_Y) and elongation at break (ϵ_B) of films, respectively. It can be recognized that σ_Y of PE/amino-POSS/FeSt₃ blend films were slightly decreased with increasing amino-POSS content (Figure 7a), while ϵ_B was moderately decreased (Figure 7b). The decrease in σ_Y and ϵ_B might be due to the presence of amino-POSS aggregates within the PE/amino-POSS/FeSt₃ blends [34].

When the films were thermally aged, their mechanical properties were decreased with the ageing time. The tensile yield strength of PE and PE/amino-POSS/FeSt₃ films was moderately decreased after

three days of thermal ageing but hardly changed afterwards. The elongation at break of pure PE film dropped to 261% and 128% from an initial figure of 265% after three and six days of thermal ageing, respectively. However, the effect of thermal exposure on the ε_B of the blend films was small. ε_B of all the aged films was more than 50% after thermal ageing.

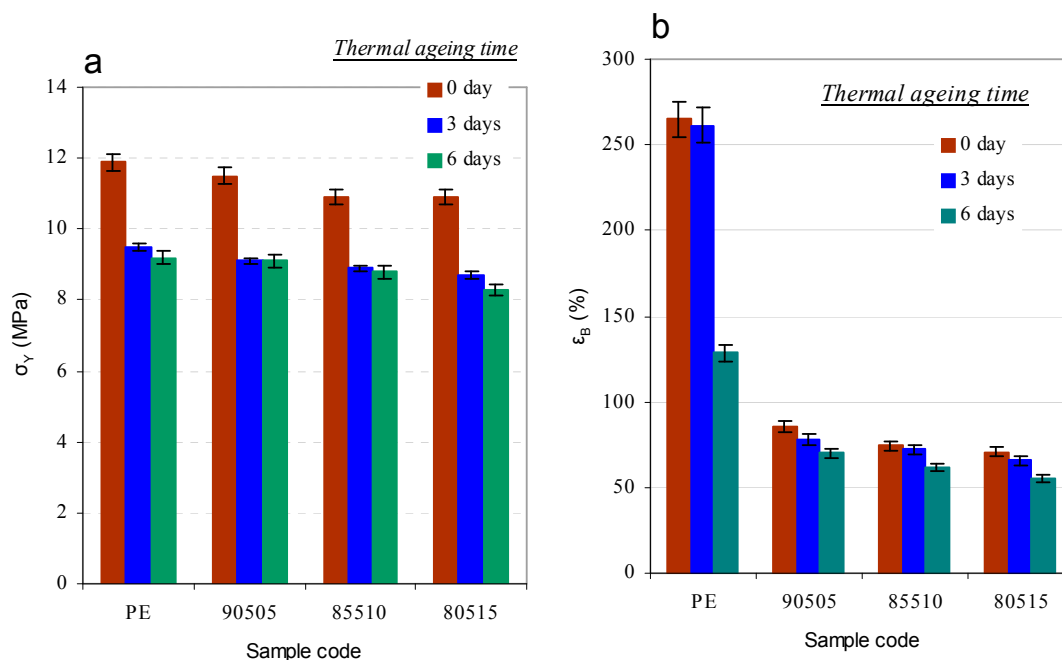


Figure 7. Effect of thermal aging on the tensile yield strength (a), an elongation at break (b) of PE/amino-POSS/FeSt₃ film.

As identified above, thermal ageing of PE/amino-POSS/FeSt₃ films led to a formation of carbonyl groups. Increasing the ageing time produced an increase in the intensity of carbonyl peak, as determined by the CI. It indicates that the polymer chains were cleaved to give a rise in carbonyl groups. Due to the cleavage of polymeric chains, ε_B also decreased as the ageing time was increased. The elongation at break was the most suitable parameter to quantify the degradation. The result of mechanical properties demonstrates that the film was degraded by thermal oxidation.

The incorporation of amino-POSS into the blends led to a larger reduction on σ_Y and ε_B of the blend films (Figure 6b). Furthermore, the presence of amino-POSS reduced the oxidation level of the blends, as the CI reduced when increasing amino-POSS content in the blends (Figure 4). It reflects that amino-POSS has an influence on the effectiveness of the pro-oxidant FeSt₃.

3.2.5. Adhesion to Paperboard

Adhesions of PE and PE/amino-POSS/FeSt₃ blends to paperboard are shown in Figure 8. As can be seen, the adhesion strength was decreased with increasing amino-POSS content while FeSt₃ content was kept constantly at 0.5 wt%. The standard deviation is relatively small for all our samples (below 50 N/m). It reflects that the adhesion strength of the blends to paperboard is equally distributed. The reduction in the adhesion with increasing amino-POSS content may be caused by a lubricant effect of the POSS compound, as previously reported [34].

When the film was thermally treated in a circulation oven, its adhesion to paperboard was altered. The adhesion strength of the aged PE to the paperboard was decreased. It was probably due to a reduction in the melt flow property of the aged PE, as determined by the MFI testing. Whereas, when PE/amino-POSS/FeSt₃ blends were thermally treated prior to coating, the adhesion to the paperboard was increased with an increase in the ageing time. Remarkably, the adhesion was improved approx. 30% by thermal treating the blend 90505 before coating on paperboard. The MFI test shows that the flowability of the blends increased with increasing the ageing time. In this case, physical interlocking could cause an enhancement in adhesion of the blends to paperboard.

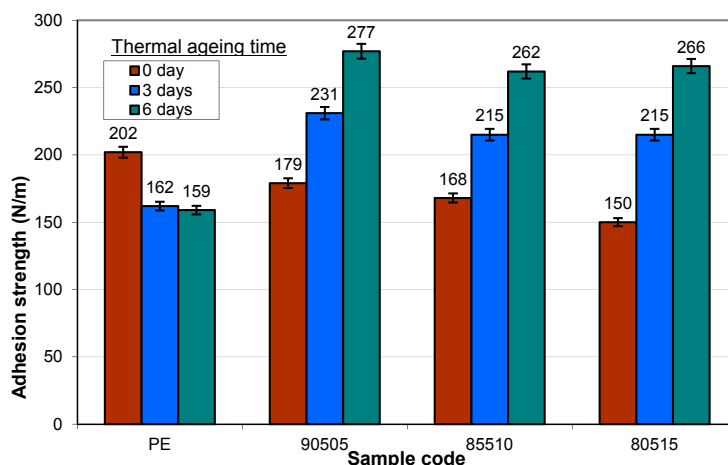


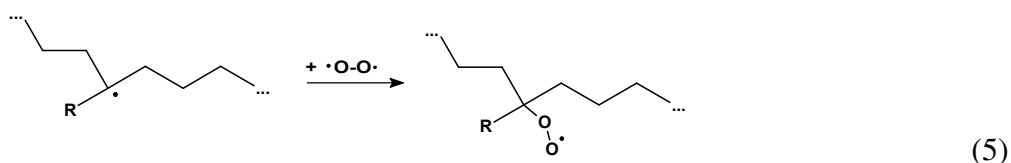
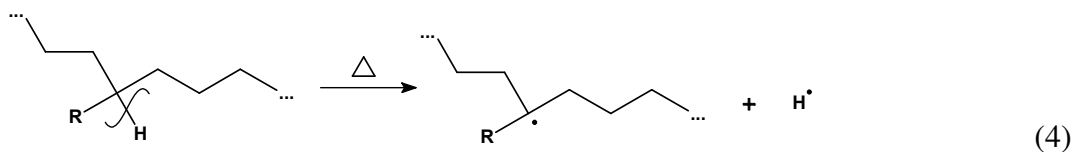
Figure 8. Adhesion strength of PE/amino-POSS/FeSt₃ blends to paperboard.

As identified by ATR-FTIR, there was a carbonyl group which formed on the surface of the PE/amino-POSS/FeSt₃ films. Such groups can interact with hydroxyl groups (OH) of the paperboard to form hydrogen bonds, as discussed previously [34]. The formation of interfacial hydrogen bonding interaction can lead to an enhancement in the adhesion of PE/amino-POSS/FeSt₃ films to paperboard.

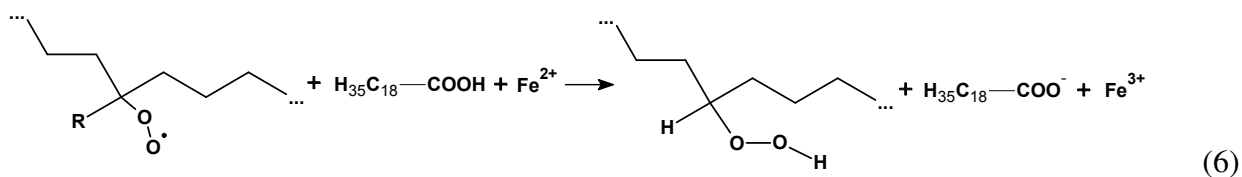
Thermal ageing and ATR-FTIR have not been done simultaneously. Sometimes, ATR-FTIR measurement has been done several days after ageing ended. The results prove that the oxidation is stable and is not eliminated due to storage. This is a big advantage compared to flame treatment or corona treatment, which lasts less than 30 min and has to be applied in-line with packaging material manufacturing.

3.2.6. Proposed Mechanism for Oxidation of PE by Iron Pro-Oxidant and Amine Accelerator

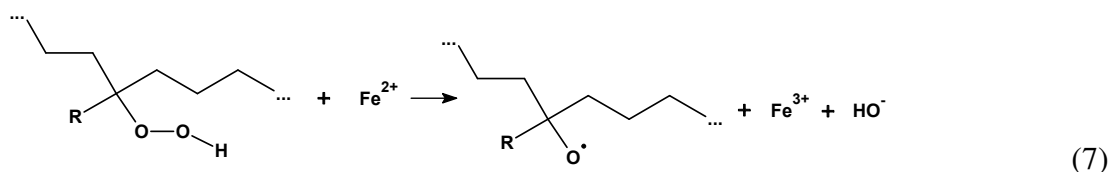
The initial steps for the oxidative degradation of polyolefins are well known:



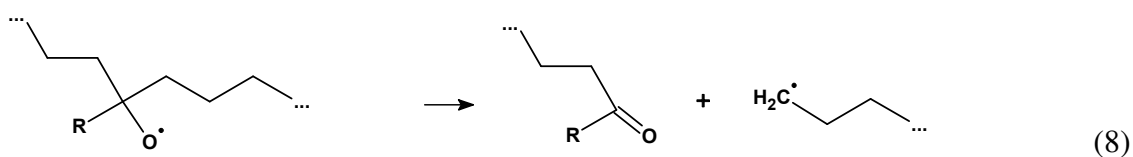
Stearic acid facilitates the transformation of peroxy radicals into hydroperoxides, which is mediated by oxidation of Fe²⁺ to Fe³⁺:



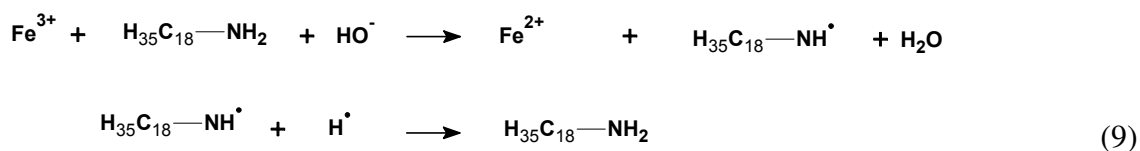
The oxidation of Fe²⁺ to Fe³⁺ is also crucial for the transformation of hydroperoxides into alkoxy radicals:



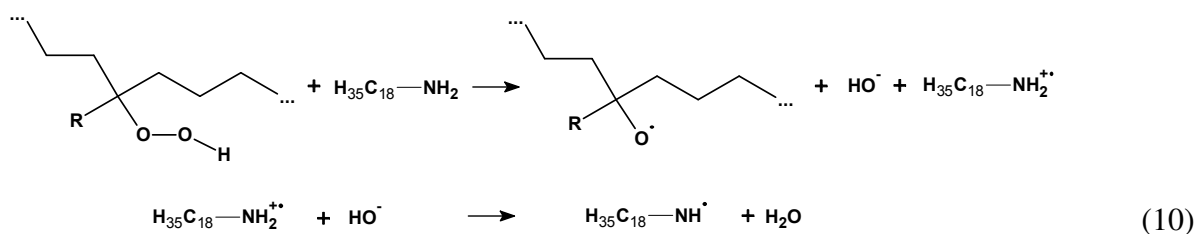
Alkoxy radicals undergo easily a bond cleavage that leads to oxidized polymer chains. Repeated chain scission in the polymer main chain leads to brittle materials.



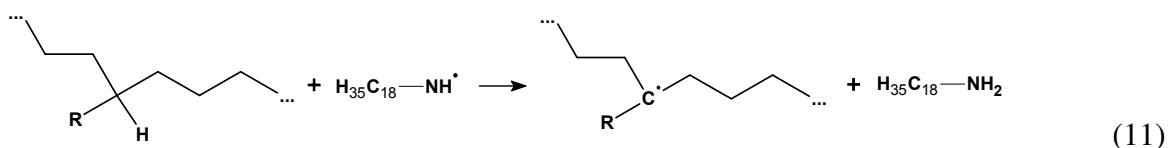
The role of the amine accelerator is on the one hand the regeneration of the iron catalyst reduction of Fe³⁺ to Fe²⁺:



On the other hand, the amine can directly lead to transformation of hydroperoxides into alkoxy radicals:



Amine radicals are capable of initiating radical formation in the PE backbone while the amine is regained.



Other reactions with the involved radicals and substances may occur, such as the combination of radicals and the reaction of radicals with different substrates. However the proposed mechanism explains the role of amine as accelerator together with an iron pro-oxidant due to acceleration of rate limiting steps. Especially, the regeneration of iron after transformation of peroxy radicals into alkoxy radicals is an important role of the amine. The proposed mechanism is in good compliance with the experimental results.

4. Conclusions

Stearyl amine and amino-POSS have been used together with ferric stearate (FeSt_3) in order to accelerate the thermal oxidation of polyolefins. Significant acceleration in thermal oxidation of polypropylene and polyethylene compared to reference materials without amine has been obtained. A mechanism has been proposed which can explain the role of amines during thermal oxidation of polyolefins. The regeneration of the iron catalyst seems to be an important role of the amine. Amino-POSS has been chosen for food packaging applications due to its expected lower leakage from PE compared with stearyl amine.

The pro-oxidant additive ferric (III) stearate and amino-POSS were introduced into PE by using a melt mixing method. The effect on the adhesion strength of the resulting PE films to paperboard has been examined. The oxidative degradation and melt flow properties of the PE were obviously affected by amine-POSS. Small amounts of amino-POSS resulted in a fast increase of the carbonyl index showing a fast oxidation. Increasing amino-POSS content did not further accelerate the oxidation. This behaviour is in good compliance with the main role of amino-POSS as regenerator of the iron catalyst. The mechanical properties (tensile yield strength and elongation at break) of PE/amino-POSS/ FeSt_3 films decreased, but the films still remained flexible. When PE/amino-POSS/ FeSt_3 films were compression moulding coated on paperboard, the adhesion strength was decreased with increasing amino-POSS content which is in good compliance with earlier findings. The adhesion was however increased when such films were treated at 70 °C prior to coating. The adhesion improvement was probably due to the interaction between OH groups of paperboard and C=O groups of PE/amino-POSS/ FeSt_3 blends. The physical interlocking due to reduced melt viscosity could be considered as a reason for adhesion improvement. Processing of coated paperboard in state-of-the-art packaging machines should be feasible.

From a commercial point of view, it is important to remember that amino-POSS is applied in small quantities and its manufacturing is based on commodities. On the other hand, the six-day thermal aging would significantly increase the costs of the final cardboard. Further work should be done in order to utilize the observed accelerated oxidation within existing packaging manufacturing processes. The persistence of the oxidation could be used in cases where short storage of films prior to lamination are part of the packaging manufacturing process. Amount of amino-POSS used, storage time and storage temperature should of course be optimized for a given process. This has been beyond the scope of the present work. In contrast to earlier work, where fatty amide substituted POSS has been used, the adhesion improvement has been obtained by an oxidation process. This aspect could open up the opportunity for application in different materials and possible enhancement of other properties such as oxygen scavenging or anti-microbial surfaces.

Acknowledgments

This study has been financially supported by the Research Council of Norway and the industrial partners Dynea AS, Elopak AS, Forestia AS, Peterson Linerboard AS, Korsnäs AB, and Södra Cell AB in the KMB project (SustainBarrier 182619). The authors are grateful for the materials received from Normatch AS (Gjerdrum) and Nor-X Industry AS (Gursken), Norway; and Korsnäs AB, Frövi, Sweden.

Author Contributions

This paper has been done by Tuan-Anh Nguyen, PhD Candidate from Department of Chemical Engineering, Norwegian University of Science and Technology (NTNU). The scientific work has been mainly supervised by Senior Scientist, Ferdinand Männle (Synthesis and Properties, SINTEF Materials and Chemistry, Oslo, Norway) and Øyvind Weiby Gregersen (The faculty of Natural Sciences and Technology, NTNU, Trondheim, Norway).

Conflicts of Interest

The authors declare no conflict of interest.

Abbreviations

Amino-POSS, [3-(11-aminoundecanoyl) amino) propane-1-] silsesquioxane; ATR-FTIR, Attenuated Total Reflectance Fourier transform infrared spectroscopy; CI, Carbonyl index; FeSt₃, Ferric stearate; MFI, Melt flow index; PE, Polyethylene; mb, masterbatch.

References

1. Kemppi, A. *Studies on the Adhesion between Paper and Low Density Polyethylene*; Åbo Akademi University: Åbo, Finland, 1997; p. 39.
2. Westerlind, B.; Larsson, A.; Rigdahl, M. Determination of the degree of adhesion in plasma-treated polyethylene/paper laminates. *Int. J. Adhes. Adhes.* **1987**, *7*, 141–146. [[CrossRef](#)]
3. Kaplan, S.L.; Rose, P.W. Plasma surface treatment of plastics to enhance adhesion. *Int. J. Adhes. Adhes.* **1991**, *11*, 109–113. [[CrossRef](#)]
4. Nikos, K. Oxobiodegradable Polyolefins: Their Biodegradation and Recycling. Available online: [http://eurasia12.uoi.gr/Abstracts_pdf/\(4\)%20Environmental%20and%20Green%20chemistry/S4%20ORAL/OP20_Abstract_Katsaros.pdf](http://eurasia12.uoi.gr/Abstracts_pdf/(4)%20Environmental%20and%20Green%20chemistry/S4%20ORAL/OP20_Abstract_Katsaros.pdf) (accessed on 11 August 2015).
5. Scott, G. Photo-biodegradable plastics: Their role in the protection of the environment. *Polym. Degrad. Stable* **1990**, *29*, 135–154. [[CrossRef](#)]
6. Roy, P.K.; Surekha, P.; Raman, R.; Rajagopal, C. Investigating the role of metal oxidation state on the degradation behaviour of LDPE. *Polym. Degrad. Stable* **2009**, *94*, 1033–1039. [[CrossRef](#)]
7. Männle, F.; Jørgensen, J.K.; Tanem, B.S. Increased performance of thermoplastic packaging materials by using a mild oxidizing biobased additive. *Int. J. Polym. Sci.* **2012**, *2012*, 297923. [[CrossRef](#)]

8. Sipinen, A.J.; Rutherford, D.R. A study of the oxidative degradation of polyolefins. *J. Environ. Polym. Degr.* **1993**, *3*, 193–202. [[CrossRef](#)]
9. Bartlett, P.D.; Nozaki, K. The kinetics of decomposition of benzoyl peroxide in solvents. *J. Am. Chem. Soc.* **1946**, *68*, 1686–1692.
10. Tobolsky, A.V.; Mesrobian, R.B. *Organic Peroxides—Their Chemistry, Decomposition and Role in Polymerization*; Interscience Publishers, Inc.: New York, NY, USA, 1954; p. 55.
11. Salem, I.A. Role of aliphatic diamine ligands in hydrogen peroxide decomposition with Dowex-50W resin as transition metal complex ions. *J. Mol. Catal.* **1993**, *80*, 11–19. [[CrossRef](#)]
12. Eyler, G.N.; Canizo, A.I.; Alvarez, E.E. Thermal decomposition of cyclic organic peroxides in aliphatic amines solution. *Afinidad Barcelona* **2007**, *64*, 538–542.
13. Tidjani, A. Comparison of formation of oxidation products during photo-oxidation of linear low density polyethylene under different natural and accelerated weathering conditions. *Polym. Degrad. Stabil.* **2000**, *68*, 465–469. [[CrossRef](#)]
14. Chiellini, E.; Corti, A.; Swift, G. Biodegradation of thermally-oxidized, fragmented low-density polyethylenes. *Polym. Degrad. Stabil.* **2003**, *81*, 341–351. [[CrossRef](#)]
15. Koutny, M.; Sancelme, M.; Dabin, C.; Pichon, N.; Delort, A.-M.; Lemaire, J. Acquired biodegradability of polyethylene containing pro-oxidant additives. *Polym. Degrad. Stabil.* **2006**, *9*, 1495–1503. [[CrossRef](#)]
16. Chiellini, E.; Corti, A.; D'Antone, S.; Baciú, R. Oxo-biodegradable carbon backbone polymers—Oxidative degradation of polyethylene under accelerated test conditions. *Polym. Degrad. Stabil.* **2006**, *91*, 2739–2747. [[CrossRef](#)]
17. Kumanayaka, T.O.; Parthasarathy, R.; Jollands, M. Accelerating effect of montmorillonite on oxidative degradation of polyethylene nanocomposites. *Polym. Degrad. Stabil.* **2010**, *95*, 672–676. [[CrossRef](#)]
18. Corti, A.; Muniyasamy, S.; Vitali, M.; Imam, S.H.; Chiellini, E. Oxidation and biodegradation of polyethylene films containing pro-oxidant additives: Synergistic effects of sunlight exposure, thermal ageing and fungal biodegradation. *Polym. Degrad. Stabil.* **2010**, *95*, 1106–1114. [[CrossRef](#)]
19. Yashchuk, O.; Portillo, F.S.; Hermida, E.B. Degradation of polyethylene film samples containing oxo-degradable additives. *Procedia Mater. Sci.* **2012**, *1*, 439–445. [[CrossRef](#)]
20. Briggs, D.; Brewis, D.M.; Konieczko, M.B. X-ray photoelectron spectroscopy studies of polymer surfaces. *J. Mater. Sci.* **1979**, *14*, 1344–1348. [[CrossRef](#)]
21. Junnila, J.; Savolainen, A.; Forsberg, D. Adhesion Improvements between Paper and Polyethylene by Pre-Treatment of Substrate. In *Polymers, Laminations and Coatings Conference*, Orlando, FL, USA, 5–8 September 1989; pp. 353–360.
22. Savolainen, A.; Kuusipalo, J. The Optimization of Corona and Flame Pre-Treatment in Multilayer Coating. In *Proceedings from the 1991 Tappi Extrusion Coating Short Course*, Düsseldorf, Germany; 1991; pp. 897–904.
23. Li, G.Z.; Wang, L.C.; Ni, H.; Pittman, C.U. Polyhedral oligomeric silsesquioxane (POSS) polymers and copolymers: A review. *J. Inorg. Organomet. Polym.* **2001**, *11*, 123–154. [[CrossRef](#)]

24. Markovic, E.; Constantopolous, K.; Matisons, J.G. Polyhedral Oligomeric Silsesquioxanes: From Early and Strategic Development through to Materials Application. In *Application of Polyhedral Ologomeric Silsequioxanes*; Hartmann-Thompson, C., Ed.; Advances in Silicon Science. Springer Netherlands: Dordrecht, The Netherlands, 2011; Volume 3, pp. 1–46.
25. Fina, A.; Tabuani, D.; Frache, A.; Camino, G. Polypropylene-polyhedral oligomeric silsesquioxanes (POSS) nanocomposites. *Polymer* **2005**, *46*, 7855–7866. [[CrossRef](#)]
26. Fina, A.; Tabuani, D.; Frache, A.; Camino, G. Polypropylene–polysilsesquioxane blends. *Eur. Polym. J.* **2010**, *46*, 14–23. [[CrossRef](#)]
27. Joshi, M.; Butola, B.S.; Simon, G.; Kukaleva, N. Rheological and viscoelastic behavior of HDPE/octamethyl-POSS nanocomposites. *Macromolecules* **2006**, *39*, 1839–1849. [[CrossRef](#)]
28. Joshi, M.; Butola, B.S. Isothermal crystallization of HDPE/octamethyl polyhedral oligomeric silsesquioxane nanocomposites: role of POSS as a nanofiller. *J. Appl. Polym. Sci.* **2007**, *105*, 978–985. [[CrossRef](#)]
29. Zhou, Z.; Zhang, Y.; Zhang, Y.; Yin, N. Rheological behavior of polypropylene/octavinyl polyhedral oligomeric silsesquioxane composites. *J. Polym. Sci. Polym. Phys.* **2008**, *46*, 526–533. [[CrossRef](#)]
30. Misra, R.; Fu, B.X.; Morgan, S.E. Surface energetics, dispersion and nanotribomechanical behavior of POSS/PP hybrid nanocomposites. *J. Polym. Sci. Polym. Phys.* **2007**, *45*, 2441–2455. [[CrossRef](#)]
31. Sánchez-Soto, M.; Schiraldi, D.A.; Illescas, S. Study of the morphology and properties of melt-mixed polycarbonate–POSS nanocomposites. *Eur. Polym. J.* **2009**, *45*, 341–352. [[CrossRef](#)]
32. Bourbigot, S.; Turf, T.; Bellayer, S.; Duquesne, S. Polyhedral oligomeric silsesquioxane as flame retardant for thermoplastic polyurethane. *Polym. Degrad. Stabil.* **2009**, *94*, 1230–1237. [[CrossRef](#)]
33. Lim, S.K.; Hong, E.P.; Choi, H.; Chin, I.J. Polyhedral oligomeric silsesquioxane and polyethylene nanocomposites and their physical characteristics. *J. Ind. Eng. Chem.* **2010**, *16*, 189–192. [[CrossRef](#)]
34. Nguyen, T.-A.; Männle, F.; Gregersen, Ø.W. Polyethylene/octa-(ethyl octadeca-10,13-dienoamide) silsesquioxane blends and the adhesion strength to paperboard. *Int. J. Adhes. Adhes.* **2012**, *38*, 117–124. [[CrossRef](#)]
35. Männle, F.; Tofteberg, T.R.; Skaugen, M.; Bu, H.; Peters, T.; Dietzel, P.D.C.; Pilz, M. Polymer nanocomposite coatings based on polyhedral oligosilsesquioxanes: Route for industrial manufacturing and barrier properties. *J. Nanopart. Res.* **2011**, *13*, 4691–4701. [[CrossRef](#)]
36. Rao, C.N.R. *Chemical Applications of Infrared Spectroscopy*; Academic Press: Waltham, MA, USA, 1963; pp. 125–263.
37. Abrahamson, H.B.; Lukaski, H.C. Synthesis and characterization of iron stearate compounds. *J. Inorg. Biochem.* **1994**, *54*, 115–130. [[CrossRef](#)]
38. Zweifel, H. *Plastic Additives Handbook*, 5th ed.; Hanser Gardner Publications: Munich, Germany, 2001; pp. 8–9.

39. Eyenga, I.I.; Focke, W.W.; Prinsloo, L.C.; Tolmay, A.T. Photodegradation: A solution for the shopping bag “visual pollution” problem? *Macromol. Symp.* **2002**, *178*, 139–152. [[CrossRef](#)]

© 2015 by the authors; licensee MDPI, Basel, Switzerland. This article is an open access article distributed under the terms and conditions of the Creative Commons Attribution license (<http://creativecommons.org/licenses/by/4.0/>).